column vector	$\boldsymbol{x}$	$|\boldsymbol{x}\rangle$
row vector	$\boldsymbol{w}^{\top}$	$\langle\boldsymbol{w}|$
scalar product	$\boldsymbol{w}^{\top}\boldsymbol{x}$	$\langle\boldsymbol{w}|\boldsymbol{x}\rangle$
rank-one matrix	$\boldsymbol{x}\boldsymbol{w}^{\top}$	$|\boldsymbol{x}\rangle\langle\boldsymbol{w}|$

For example, the equality $\boldsymbol{w}^{\top}A\boldsymbol{x} = \boldsymbol{w}^{\top}(A\boldsymbol{x}) = (A^{\top}\boldsymbol{w})^{\top}\boldsymbol{x}$ corresponds to $\langle\boldsymbol{w}|A|\boldsymbol{x}\rangle = \langle\boldsymbol{w}|A\boldsymbol{x}\rangle = \langle A^{\top}\boldsymbol{w}|\boldsymbol{x}\rangle$ in the new notation.

Appendix A. Generic perturbations lead to the same asymptotic return rate

Here we show that the asymptotic return rates are essentially independent of the perturbation direction $\boldsymbol{u}$ and of the observation direction $\boldsymbol{w}$.

We begin by investigating the long-term behavior of $\langle\boldsymbol{w},\boldsymbol{x}(t)\rangle = \langle\boldsymbol{w}, \mathrm{e}^{At}\boldsymbol{u}\rangle$. We assume that A has no degenerate eigenvalues, which is generically the case. This ensures that its spectral decomposition exists, constructed using the eigenvalues λ_i and corresponding (right) eigenvectors $\boldsymbol{v}_i^{\mathrm{R}}$ and left eigenvectors $\boldsymbol{v}_i^{\mathrm{L}}$ (i.e., eigenvectors of $A^{\top}$). For simplicity we assume that the dominant eigenvalue is real; we discuss the case of a complex conjugate pair of dominant eigenvalues at the end of this appendix. We order the eigenvalues such that

$$\lambda_1 > \mathfrak{Re}(\lambda_2) \geq \mathfrak{Re}(\lambda_3) \geq \dots$$

Using the spectral decomposition, we have

$$A = \sum_i \lambda_i|\boldsymbol{v}_i^{\mathrm{R}}\rangle\langle\boldsymbol{v}_i^{\mathrm{L}}| \quad \text{and} \quad \mathrm{e}^{At} = \sum_i \mathrm{e}^{\lambda_i t}|\boldsymbol{v}_i^{\mathrm{R}}\rangle\langle\boldsymbol{v}_i^{\mathrm{L}}|,$$

so that

$$\langle\boldsymbol{w}|\boldsymbol{x}(t)\rangle = \langle\boldsymbol{w}|\mathrm{e}^{At}\boldsymbol{u}\rangle = \sum_i \mathrm{e}^{\lambda_i t}\langle\boldsymbol{w}|\boldsymbol{v}_i^{\mathrm{R}}\rangle\langle\boldsymbol{v}_i^{\mathrm{L}}|\boldsymbol{u}\rangle.$$

If $\langle\boldsymbol{w}|\boldsymbol{v}_1^{\mathrm{R}}\rangle\langle\boldsymbol{v}_1^{\mathrm{L}}|\boldsymbol{u}\rangle \neq 0$ and for sufficiently large t (more precisely, for $\mathrm{e}^{-(\lambda_1 - \mathfrak{Re}(\lambda_2))t} \ll 1$), the sum in the right-hand side is dominated by the $i = 1$ term,

$$\langle\boldsymbol{w}|\boldsymbol{x}(t)\rangle \approx \mathrm{e}^{\lambda_1 t}\langle\boldsymbol{w}|\boldsymbol{v}_1^{\mathrm{R}}\rangle\langle\boldsymbol{v}_1^{\mathrm{L}}|\boldsymbol{u}\rangle,$$

so that (see also Appendix B),

$$-\frac{\ln|\langle\boldsymbol{w}|\boldsymbol{x}(t)\rangle|}{t} \approx -\lambda_1 - \frac{\ln|\langle\boldsymbol{w}|\boldsymbol{v}_1^{\mathrm{R}}\rangle\langle\boldsymbol{v}_1^{\mathrm{L}}|\boldsymbol{u}\rangle|}{t} \approx -\lambda_1$$

$$\mathcal{R}_t^{\mathrm{ins}}(\boldsymbol{w}) = -\frac{\mathrm{d}}{\mathrm{d}t}\ln|\langle\boldsymbol{w}|\boldsymbol{x}(t)\rangle| \approx -\lambda_1 - \frac{\mathrm{d}}{\mathrm{d}t}\ln|\langle\boldsymbol{w}|\boldsymbol{v}_1^{\mathrm{R}}\rangle\langle\boldsymbol{v}_1^{\mathrm{L}}|\boldsymbol{u}\rangle| = -\lambda_1$$

$$\mathcal{R}_t^{\mathrm{avg}}(\boldsymbol{w}) = -\frac{\ln|\langle\boldsymbol{w}|\boldsymbol{x}(t)\rangle| - \ln|\langle\boldsymbol{w}|\boldsymbol{x}(0)\rangle|}{t} \approx -\lambda_1.$$

These approximations, valid for large t, become exact in the limit $t \to \infty$. Hence,

$$\mathcal{R}_\infty(\boldsymbol{w}) = \lim_{t\to\infty}\mathcal{R}_t^{\mathrm{ins}}(\boldsymbol{w}) = \lim_{t\to\infty}\mathcal{R}_t^{\mathrm{avg}}(\boldsymbol{w}) = -\lambda_1.$$

Hence, the asymptotic return rates do not depend on the perturbation direction $\boldsymbol{u}$ (as long as $\langle\boldsymbol{v}_1^{\mathrm{L}}|\boldsymbol{u}\rangle \neq 0$) and on the observation direction $\boldsymbol{w}$ (as long as $\langle\boldsymbol{w}|\boldsymbol{v}_1^{\mathrm{R}}\rangle \neq 0$).

Similarly, for sufficiently large t and if $\langle\boldsymbol{v}_1^{\mathrm{L}}|\boldsymbol{u}\rangle \neq 0$,

$$\|\boldsymbol{x}(t)\| \approx \mathrm{e}^{\lambda_1 t}\|\boldsymbol{v}_i^{\mathrm{R}}\|\langle\boldsymbol{v}_i^{\mathrm{L}}|\boldsymbol{u}\rangle.$$

Substituting this expression into the defintion of return rates $\mathcal{R}_\infty$, $\mathcal{R}_t^{\mathrm{ins}}$ and $\mathcal{R}_t^{\mathrm{avg}}$, we get

$$\mathcal{R}_\infty = \lim_{t\to\infty}\mathcal{R}_t^{\mathrm{ins}} = \lim_{t\to\infty}\mathcal{R}_t^{\mathrm{avg}} = -\lambda_1.$$

The case of a complex conjugate pair of dominant eigenvalues is more subtle. In this case also the asymptotic return to equilibrium is governed by the dominant pair of eigenvalues (and corresponding eigenvectors). The asymptotic regime has persistent oscillations of decreasing amplitude. The rate of decrease of the amplitude is equal to asymptotic resilience (equal to minus the real part of the
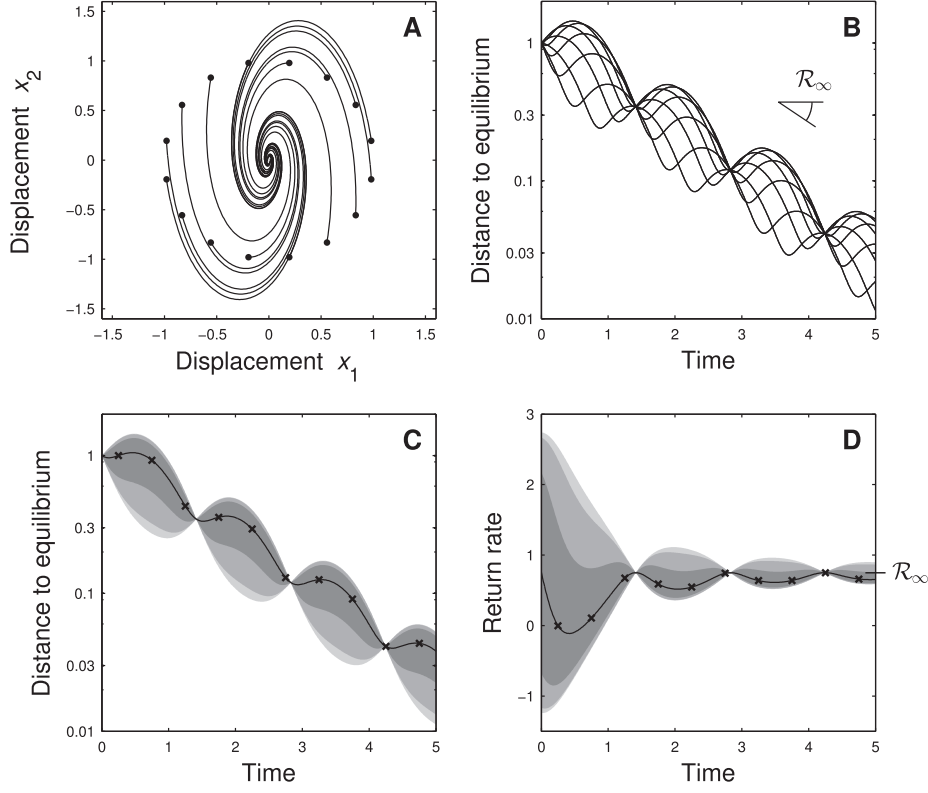
Appendix

"Bra-ket" notation In the appendices we use special notation to deal with column vectors, row vectors and their products. The correspondence between this notation, which is borrowed from theoretical physics, and the more standard one is:

Fig. A.1. Return to equilibrium depends on perturbation direction - case of complex conjugate pair of dominant eigenvalues. Same figure as Fig. 3, but for different community matrix, $A = \begin{pmatrix} -0.5 & -1 \\ 5 & -1 \end{pmatrix}$. The oscillatory behavior leaves a clear imprint on the decay of the distance to equilibrium (panel C) and on the convergence of return rate $\mathcal{R}_t^{\text{avg}}$ to asymptotic resilience (panel D).

dominant eigenvalues). However, because the return rates are computed on the oscillating variables (rather than on the amplitude of the oscillations), the return rates for large t can also oscillate, without converging to a proper limit. The distribution of instantaneous return rates $\mathcal{R}_t^{\text{ins}}$ remains wide for large time t (Fig. A.1). In contrast, the average return rates $\mathcal{R}_t^{\text{avg}}$ have a distribution that becomes narrow for large time t, converging to asymptotic resilience.

Appendix B. Direction of observation

In the main text we defined return rates using the Euclidean norm $\|\boldsymbol{x}(t)\|$ to measure the extent of the dynamical displacement from equilibrium, see Eqs. (3)–(5). To compute the associated return rates, all dynamical variables $x_i(t)$ have to be observed. When this is not practical or even possible, it is more convenient to use return rates that require a limited number of dynamical variables. Here we introduce return rates of a particular ecosystem variable of function (e.g., total biomass, nutrient uptake). After linearization such a variable becomes a linear combination $\sum_i w_i x_i(t) = \boldsymbol{w}^\top \boldsymbol{x} = \langle \boldsymbol{w} | \boldsymbol{x} \rangle$, where the vector $\boldsymbol{w}$ can be interpreted as an observation direction. For instance, the direction of total biomass is $\boldsymbol{w}^\top = (1, 1, \ldots, 1)$. The corresponding return rates are

$$\mathcal{R}_\infty(\boldsymbol{w}) = \lim_{t \to \infty} -\frac{\ln|\langle \boldsymbol{w}|\boldsymbol{x}(t)\rangle|}{t} \tag{B.1}$$

$$\mathcal{R}_t^{\text{ins}}(\boldsymbol{w}) = -\frac{\mathrm{d}}{\mathrm{d}t} \ln|\langle \boldsymbol{w}|\boldsymbol{x}(t)\rangle| \tag{B.2}$$

$$\mathcal{R}_t^{\text{avg}}(\boldsymbol{w}) = -\frac{\ln|\langle \boldsymbol{w}|\boldsymbol{x}(t)\rangle| - \ln|\langle \boldsymbol{w}|\boldsymbol{x}(0^+)\rangle|}{t}. \tag{B.3}$$

Note that we have added the dependence on the observation direction $\boldsymbol{w}$ to distinguish these return rates (e.g., $\mathcal{R}_t^{\text{avg}}(\boldsymbol{w})$) from those based on the Euclidean norm (e.g., $\mathcal{R}_t^{\text{avg}}$).

Appendix C. Return times

As explained in the main text, return time can be defined as the amount of time it takes for the system to return, and remain within, a specified distance to equilibrium. We denote the allowed distance to equilibrium by c. Then, the return time $T(c)$ is defined as

$$T(c) = \min\left\{t \mid \|\boldsymbol{x}(t+s)\| \leq c \text{ for all } s \geq 0\right\}. \tag{C.1}$$

Fig. C.1 illustrates how the requirement that the displacement remains within this bound for all times $t \geq T(c)$ allows us to deal with non-monotonous return to equilibrium. It is interesting to note that the inverse function $T(c)$ has a simple interpretation. It is the maximal displacement $C(t)$ that occurs after time t,

$$C(t) = \max_{s \geq t} \|\boldsymbol{x}(s)\|. \tag{C.2}$$

The relationship between $T(c)$ and $C(t)$ is explained graphically in Fig. C.1.

Neither $T(c)$ nor $C(t)$ are directly comparable to return rates $\mathcal{R}_t^{\text{ins}}$ and $\mathcal{R}_t^{\text{avg}}$. To see this, note that $T(c)$ has units of time, while $C(t)$ is unitless (recall that $\mathcal{R}_t^{\text{ins}}$ and $\mathcal{R}_t^{\text{avg}}$ have units of reciprocal time). This shortcoming can be overcome by applying an appropriate transformation to $T(c)$ and $C(t)$. To find this transformation, we consider a single-species system, for which $A = -\alpha$ with $\alpha > 0$ and $\mathcal{R}_t^{\text{ins}} = \mathcal{R}_t^{\text{avg}} = \alpha$. We find $C(t) = x(0^+) e^{-\alpha t}$ and $T(c) = -(\ln c - \ln x(0^+))/\alpha$, suggesting the following transformed quanti-
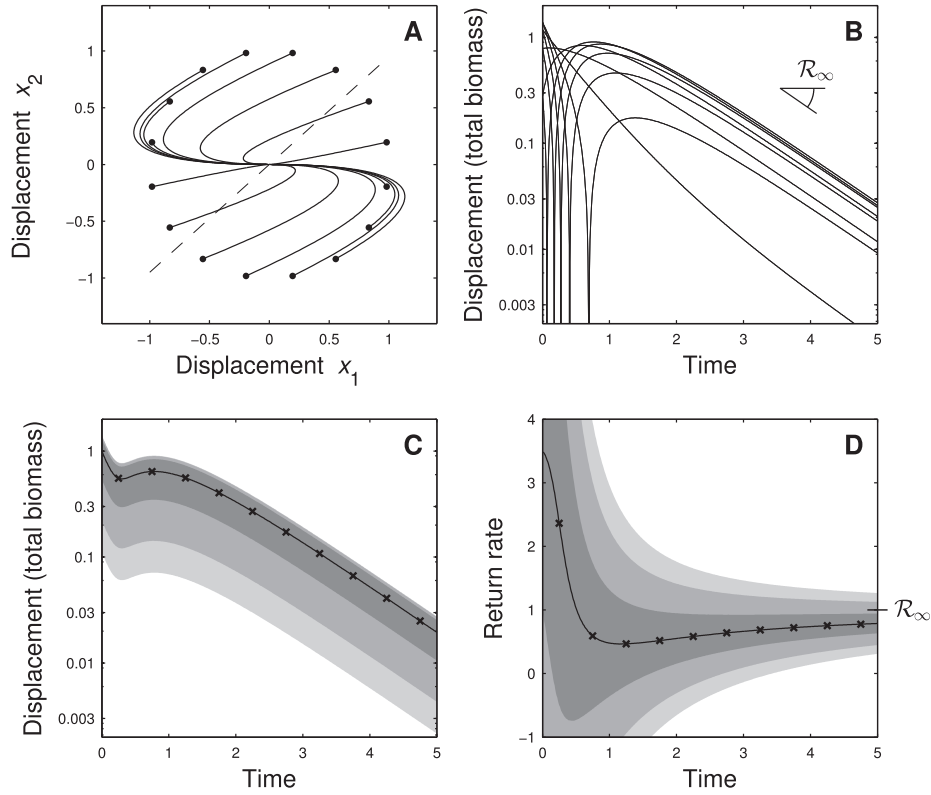
Fig. B.1. Return to equilibrium depends on perturbation direction - displacement measured along a particular observation direction. Same figure as Fig. 3, but the displacement from equilibrium is measured as the deviation of total biomass from its equilibrium value. This corresponds to projecting the trajectories on the observation direction $\boldsymbol{w}^\top = (1, 1)$ (dashed line in panel A). The patterns are qualitatively the same as those in Fig. 3, but the variation around the median is larger.
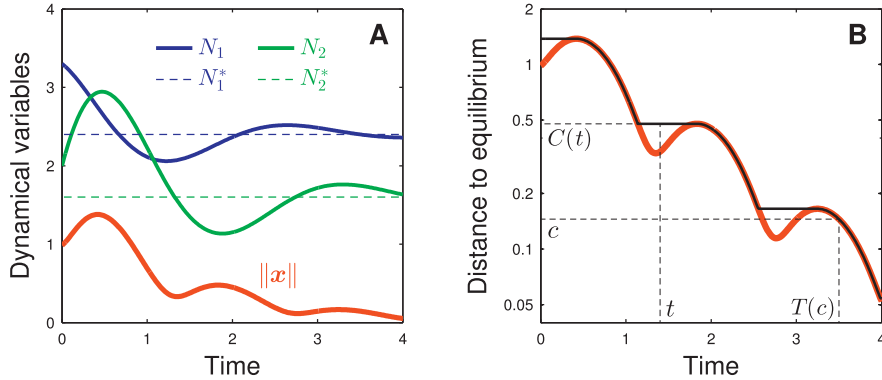

Fig. C.1. Definition of return times. Panel A: same as Fig. 1, but for a return to equilibrium with damped oscillations. Panel B: we define the return time $T(c)$ as the smallest time starting from which the distance to equilibrium remains smaller than a factor c of the initial displacement $\|\boldsymbol{x}(0^+)\|$. To construct the return time, it is convenient to introduce the quantity $C(t)$ as the largest displacement after time t relative to the initial displacement. The function $C(t)$ is monotonously decreasing; its inverse is the return time $T(c)$. Parameter values: $\boldsymbol{N}^{*\top} = (2.4, 1.6)$, $A = \begin{pmatrix} -0.5 & -1 \\ 5 & -1 \end{pmatrix}$ and $\boldsymbol{u}^\top = (0.9, 0.4)$.

ties,

$$\mathcal{C}_t = -\frac{\ln C(t) - \ln \|\boldsymbol{x}(0^+)\|}{t} \quad \text{and} \quad \mathcal{T}_c = -\frac{\ln c - \ln \|\boldsymbol{x}(0^+)\|}{T(c)},$$

(C.3)

which have the dimension of reciprocal time. For the purpose of comparison, stability measure $\mathcal{C}_t$ is of particular interest, because it is indexed by time t like return rates $\mathcal{R}_t^{\text{ins}}$ and $\mathcal{R}_t^{\text{avg}}$. Substituting the definition of $C(t)$, we get

$$\mathcal{C}_t = -\frac{\ln \max_{s \geq t} \|\boldsymbol{x}(s)\| - \ln \|\boldsymbol{x}(0^+)\|}{t},$$

showing that $\mathcal{C}_t$ is closely related to $\mathcal{R}_t^{\text{avg}}$. They are equal when $\max_{s \geq t} \|\boldsymbol{x}(s)\| = \|\boldsymbol{x}(t)\|$, which holds when the return to equilibrium is monotonous. This indicates that our results, although mostly expressed in terms of return rate $\mathcal{R}_t^{\text{avg}}$, are also valid for stability measures based on return times such as $\mathcal{C}_t$.

Appendix D. Median return rate

We derive approximate expressions for the median value of return rates $\mathcal{R}_t^{\text{ins}}$ and $\mathcal{R}_t^{\text{avg}}$ for a random perturbation $\boldsymbol{u}$. The only information the approximation requires about the distribution of perturbation vectors $\boldsymbol{u}$ is a correlation matrix C. In the next section

we compute this correlation matrix for a few simple perturbation models.

We start by deriving some exact expressions for averages over the distribution of perturbation vectors. First, we consider the squared displacement from equilibrium. Denoting by $\mathbb{E}$ the mean over the distribution of vectors $\boldsymbol{u}$, we have

$$
\begin{aligned}
\mathbb{E}\left(\|\boldsymbol{x}(t)\|^2\right) &= \mathbb{E}\langle\boldsymbol{x}(t)|\boldsymbol{x}(t)\rangle \\
&= \mathbb{E}\langle e^{At}\boldsymbol{u}|e^{At}\boldsymbol{u}\rangle \\
&= \mathbb{E}\left(\operatorname{Tr}|e^{At}\boldsymbol{u}\rangle\langle e^{At}\boldsymbol{u}|\right) \\
&= \operatorname{Tr} e^{At}\mathbb{E}\left(|\boldsymbol{u}\rangle\langle\boldsymbol{u}|\right)e^{A^\top t} \\
&= \operatorname{Tr} e^{At} C e^{A^\top t},
\end{aligned} \tag{D.1}
$$

where $C = \mathbb{E}|\boldsymbol{u}\rangle\langle\boldsymbol{u}|$ is the correlation matrix of perturbation vectors.

Next, we consider the time derivative of the squared displacement from equilibrium. We have

$$
\begin{aligned}
\frac{d}{dt}\|\boldsymbol{x}(t)\|^2 &= \frac{d}{dt}\langle e^{At}\boldsymbol{u}|e^{At}\boldsymbol{u}\rangle \\
&= \langle A\boldsymbol{x}(t)|x(t)\rangle + \langle\boldsymbol{x}(t)|A\boldsymbol{x}(t)\rangle \\
&= 2\langle\boldsymbol{x}(t)|H(A)\boldsymbol{x}(t)\rangle,
\end{aligned}
$$

where $H(A) = (A + A^\top)/2$ is the symmetric part of matrix A. Taking the mean over the perturbation vectors $\boldsymbol{u}$,

$$
\begin{aligned}
\mathbb{E}\left(\frac{d}{dt}\|\boldsymbol{x}(t)\|^2\right) &= 2\,\mathbb{E}\langle\boldsymbol{x}(t)|H(A)\boldsymbol{x}(t)\rangle \\
&= 2\,\mathbb{E}\left(\operatorname{Tr}|H(A)e^{At}\boldsymbol{u}\rangle\langle e^{At}\boldsymbol{u}|\right) \\
&= 2\operatorname{Tr} H(A)e^{At}\mathbb{E}\left(|\boldsymbol{u}\rangle\langle\boldsymbol{u}|\right)e^{A^\top t} \\
&= 2\operatorname{Tr} H(A)e^{At}C e^{A^\top t}.
\end{aligned} \tag{D.2}
$$

We are interested in averages of $\|\boldsymbol{x}(t)\|$, $\mathcal{R}_t^{\text{ins}}$ and $\mathcal{R}_t^{\text{avg}}$. These quantities can be expressed as non-linear functions of $\|\boldsymbol{x}(t)\|^2$ and $\frac{d}{dt}\|\boldsymbol{x}(t)\|^2$,

$$
\|\boldsymbol{x}(t)\| = \sqrt{\|\boldsymbol{x}(t)\|^2}
$$

$$
\mathcal{R}_t^{\text{ins}} = -\frac{1}{2\|\boldsymbol{x}(t)\|^2}\frac{d}{dt}\|\boldsymbol{x}(t)\|^2
$$

$$
\mathcal{R}_t^{\text{avg}} = -\frac{\ln\|\boldsymbol{x}(t)\|^2 - \ln\|\boldsymbol{x}(0)\|^2}{2t}.
$$

Applying these functions to the means of $\|\boldsymbol{x}(t)\|^2$ and $\frac{d}{dt}\|\boldsymbol{x}(t)\|^2$ (i.e., Eqs. (D.1) and (D.2)) gives poor approximations for the means of $\|\boldsymbol{x}(t)\|$, $\mathcal{R}_t^{\text{ins}}$ and $\mathcal{R}_t^{\text{avg}}$. Applying the same procedure to medians leads to much better approximations. Explicitly, denoting by $\mathbb{M}$ the median value over the perturbation vectors $\boldsymbol{u}$, we get from Eqs. (D.1) and (D.2),

$$
\mathbb{M}\left(\|\boldsymbol{x}(t)\|^2\right) \approx \operatorname{Tr} C e^{A^\top t} e^{At}
$$

$$
\mathbb{M}\left(\frac{d}{dt}\|\boldsymbol{x}(t)\|^2\right) \approx 2\operatorname{Tr} C e^{A^\top t} H(A) e^{At}.
$$

Hence,

$$
\mathbb{M}\left(\|\boldsymbol{x}(t)\|\right) \approx \sqrt{\operatorname{Tr}\left(C e^{A^\top t} e^{At}\right)} \tag{D.3}
$$

$$
\mathbb{M}\left(\mathcal{R}_t^{\text{ins}}\right) \approx -\frac{\operatorname{Tr}\left(C e^{A^\top t} H(A) e^{At}\right)}{\operatorname{Tr}\left(C e^{A^\top t} e^{At}\right)} \tag{D.4}
$$

$$
\mathbb{M}\left(\mathcal{R}_t^{\text{avg}}\right) \approx -\frac{\ln\left(\operatorname{Tr} C e^{A^\top t} e^{At}\right) - \ln\left(\operatorname{Tr} C\right)}{2t}. \tag{D.5}
$$

The accuracy of the approximations is excellent, as illustrated in Figs. 2–4 and A.1 (compare full line (numerically computed median) and $\times$-marks (analytical approximation); Eq. (D.3) in panel C and Eq. (D.5) in panel D).

It is interesting to consider the median of initial return rate $\mathcal{R}_0^{\text{ins}} = \lim_{t\to 0}\mathcal{R}_t^{\text{avg}}$. From Eq. (D.4) or (D.5),

$$
\mathbb{M}\left(\mathcal{R}_0^{\text{ins}}\right) = \lim_{t\to 0}\mathbb{M}\left(\mathcal{R}_t^{\text{avg}}\right) \approx -\frac{\operatorname{Tr}\left(CH(A)\right)}{\operatorname{Tr} C} = -\frac{\operatorname{Tr}\left(CA\right)}{\operatorname{Tr} C}.
$$

In the simple case where C is proportional to the identity matrix (see next section), we find that

$$
\mathbb{M}\left(\mathcal{R}_0^{\text{ins}}\right) = \lim_{t\to 0}\mathbb{M}\left(\mathcal{R}_t^{\text{avg}}\right) = -\frac{1}{n}\operatorname{Tr} A = -\frac{1}{n}\sum_{i=1}^{n}\lambda_i = \frac{1}{n}\sum_{i=1}^{n}-\mathfrak{Re}(\lambda_i),
$$

where λ_i are the eigenvalues of A. Hence, the median initial return rate is always positive and larger than asymptotic resilience. This is the case even for reactive systems, for which the initial return rate for some perturbation directions is negative (that is, the system initially moves away from equilibrium).

A similar procedure as above can be used to derive approximations for the median values of $|\langle\boldsymbol{w}, \boldsymbol{x}(t)\rangle|$, $\mathcal{R}_t^{\text{ins}}(\boldsymbol{w})$ and $\mathcal{R}_t^{\text{avg}}(\boldsymbol{w})$,

$$
\mathbb{M}\left(|\langle\boldsymbol{w}, \boldsymbol{x}(t)\rangle|\right) \approx \sqrt{\langle w|e^{At} C e^{A^\top t} w\rangle} \tag{D.6}
$$

$$
\mathbb{M}\left(\mathcal{R}_t^{\text{ins}}(\boldsymbol{w})\right) \approx -\frac{\langle w|e^{At}\left(AC + CA^\top\right)e^{A^\top t}w\rangle}{2\langle w|e^{At} C e^{A^\top t} w\rangle} \tag{D.7}
$$

$$
\mathbb{M}\left(\mathcal{R}_t^{\text{avg}}(\boldsymbol{w})\right) \approx -\frac{\ln\langle w|e^{At} C e^{A^\top t} w\rangle - \ln\langle w|C w\rangle}{2t}. \tag{D.8}
$$

The accuracy of these approximations is illustrated in Fig. B.1 (Eq. (D.6) in panel C and Eq. (D.8) in panel D).

Appendix E. Correlation matrix of perturbations

The statistics of the perturbation $\boldsymbol{u}$ acting on the system are summarized in the correlation matrix C. Here we derive this covariance matrix for two simple random perturbation models. In the first model we assume that all perturbation directions $\boldsymbol{u}$ are equally probable. This implies that on average all species are equally displaced. In the second model we allow that certain perturbation directions are more probable than others. In particular, we assume that a typical perturbation will displace more, in absolute terms, species with large equilibrium biomass.

To define the first model, we specify the distribution of the random perturbation vector $\boldsymbol{u}$. For a given perturbation direction (i.e., given $\boldsymbol{u}/\|\boldsymbol{u}\|$), the norm $\|\boldsymbol{u}\|$ of the perturbation vector has no effect on the return rates by linearity. Hence, we can choose $\|\boldsymbol{u}\| = 1$. Then, because all perturbation directions are equally probable, we see that the perturbation vector $\boldsymbol{u}$ is uniformly distributed on the unit sphere (i.e., the sphere defined by the condition $\|\boldsymbol{u}\| = 1$).

To generate samples from this distribution, the following procedure can be used,

1. Generate a vector $\boldsymbol{v}$, of the same dimension as $\boldsymbol{u}$, consisting of independent standard Gaussian variables v_i.
2. The normalized vector $\boldsymbol{u} = \boldsymbol{v}/\|\boldsymbol{v}\|$ gives a sample from the uniform distribution on the unit sphere.

Note that the components v_i of vector $\boldsymbol{v}$ have to be taken from a Gaussian distribution for this procedure to work. Hence, we have the following relationships between the probability distributions of $\boldsymbol{v}$, $\boldsymbol{u}$ and $r = \|\boldsymbol{v}\|$,

$$
\mathbb{P}(\boldsymbol{v} \in d\boldsymbol{v}) = \mathbb{P}(r \in dr)\,\mathbb{P}(\boldsymbol{u} \in d\boldsymbol{u}) = \prod_i \mathbb{P}(v_i \in dv_i), \tag{E.1}
$$

where the distributions $\mathbb{P}(v_i \in \mathrm{d}v_i)$ are standard Gaussian.

To compute the corresponding correlation matrix C, we start from the equality

$$C = \mathbb{E} \, |\boldsymbol{u}\rangle\langle\boldsymbol{u}| = \int |\boldsymbol{u}\rangle\langle\boldsymbol{u}| \, \mathbb{P}(\boldsymbol{u} \in \mathrm{d}\boldsymbol{u}). \qquad (E.2)$$

We multiply both sides of the equation by r^2 and integrate with respect to distribution of $r = \|\boldsymbol{v}\|$. For the left-hand side, we get

$$\begin{aligned}
\int C \, r^2 \, \mathbb{P}(r \in \mathrm{d}r) &= C \int r^2 \, \mathbb{P}(r \in \mathrm{d}r) \\
&= C \int \|v\|^2 \, \mathbb{P}(\boldsymbol{v} \in \mathrm{d}\boldsymbol{v}) \\
&= C \int \sum_i v_i^2 \prod_i \mathbb{P}(v_i \in \mathrm{d}v_i) \\
&= C \sum_i \int v_i^2 \, \mathbb{P}(v_i \in \mathrm{d}v_i) = nC,
\end{aligned}$$

where n is the dimension of $\boldsymbol{u}$ and $\boldsymbol{v}$. For the right-hand side, we get

$$\int |\boldsymbol{u}\rangle\langle\boldsymbol{u}| \, \mathbb{P}(\boldsymbol{u} \in \mathrm{d}\boldsymbol{u}) \, r^2 \, \mathbb{P}(r \in \mathrm{d}r) = \int |\boldsymbol{v}\rangle\langle\boldsymbol{v}| \, \mathbb{P}(\boldsymbol{v} \in \mathrm{d}\boldsymbol{v}).$$

Hence, we find that

$$C = \frac{1}{n} \int |\boldsymbol{v}\rangle\langle\boldsymbol{v}| \, \mathbb{P}(\boldsymbol{v} \in \mathrm{d}\boldsymbol{v}). \qquad (E.3)$$

The integral in the right-hand side is equal to the correlation matrix of the random variables v_i. They are independent and have variance 1, so that

$$C = \frac{1}{n} \mathbb{1}, \qquad (E.4)$$

where $\mathbb{1}$ denotes the $n \times n$ identity matrix.

To define the second model, we give the procedure to sample random perturbations $\boldsymbol{u}$. The procedure is a slightly modified version of the previous sampling procedure,

1. Generate a vector $\boldsymbol{v}$, of the same dimension as $\boldsymbol{u}$, consisting of independent standard Gaussian variables v_i.
2. Multiply the vector $\boldsymbol{v}$ by D, the diagonal matrix containing the equilibrium species biomass, giving $\boldsymbol{w} = D\boldsymbol{v}$.
3. The normalized vector $\boldsymbol{u} = \boldsymbol{w}/\|\boldsymbol{w}\|$ gives a sample from the distribution of perturbation $\boldsymbol{u}$.

Note that this is again a distribution on the unit sphere (defined by $\|\boldsymbol{u}\| = 1$). However, this distribution is not uniform due to the multiplication by matrix D.

We compute the corresponding correlation matrix C. First, we note that the components of vector $\boldsymbol{w}$ are independent Gaussian variables. Their distributions are not identical; component w_i has variance D_{ii}^2 (and mean 0). Introducing the variable $r = \|\boldsymbol{w}\|$, we have the following relationships,

$$\mathbb{P}(\boldsymbol{w} \in \mathrm{d}\boldsymbol{w}) = \mathbb{P}(r \in \mathrm{d}r) \, \mathbb{P}(\boldsymbol{u} \in \mathrm{d}\boldsymbol{u}) = \prod_i \mathbb{P}(w_i \in \mathrm{d}w_i), \qquad (E.5)$$

Then, we can apply a similar computation as for the first model. Using that

$$\int r^2 \, \mathbb{P}(r \in \mathrm{d}r) = \sum_i \int w_i^2 \, \mathbb{P}(w_i \in \mathrm{d}w_i) = \sum_i D_{ii}^2,$$

we get

$$C = \frac{1}{\sum_i D_{ii}^2} \int |\boldsymbol{w}\rangle\langle\boldsymbol{w}| \, \mathbb{P}(\boldsymbol{w} \in \mathrm{d}\boldsymbol{w}). \qquad (E.6)$$

The integral in the right-hand side is the covariance matrix of the random variables w_i. Substituting their variances and covariances,

we find that

$$C = \frac{1}{\sum_i D_{ii}^2} D^2. \qquad (E.7)$$

This result show that, on average, species with larger biomass are affected more strongly by the perturbation. The standard deviation of the displacement of species i is proportional to D_{ii}. Hence, the displacement strength relative to species biomass does not differ between species. Note that also for this second model the perturbation affects species in an uncorrelated way.

Appendix F. Effect of rare species on asymptotic resilience

Here we illustrate a simple mechanism of how a rare species can determine asymptotic resilience. We assume that the rare species is present in the community without significantly affecting the other species, but is kept at low abundance by interactions with the core community (a satellite species). We consider two cases: one in which the rare species can persist in the community without immigration, and another in which the rare species is maintained by immigration (a sink population).

We focus on the dynamics of the satellite species, which we describe by logistic growth with immigration. Denoting its biomass by N_1, the dynamical equation reads,

$$\frac{\mathrm{d}N_1}{\mathrm{d}t} = r_1 N_1 \left(1 - \frac{N_1 + \beta_{10} N_0}{K_1}\right) + c_1, \qquad (F.1)$$

with r_1 the intrinsic growth rate, K_1 the carrying capacity, and c_1 the immigration rate of the satellite species. Variable N_0 aggregates the biomass of the core species. Because the effect of the satellite species on the core species is assumed to be negligible, the dynamics of N_0 are autonomous, converging to an equilibrium value N_0^*. Competition coefficient β_{10} quantifies the negative effect of the core species on the satellite species, effectively reducing its intrinsic growth rate,

$$r_1 \;\rightarrow\; r_1 \left(1 - \frac{\beta_{10} N_0^*}{K_1}\right) = \alpha_1 r_1 \quad \text{with} \quad \alpha_1 = 1 - \frac{\beta_{10} N_0^*}{K_1}. \qquad (F.2)$$

The factor α_1 is smaller than one, and can even be negative. The effective growth rate $\alpha_1 r_1$ is equal to the invasion fitness of the satellite species (without immigration).

First, assume the satellite species has positive invasion fitness, $\alpha_1 > 0$, so that it can persist in the community without immigration. Neglecting immigration, $c_1 = 0$, we find that the equilibrium biomass is $N_1^* = \alpha_1 K_1$ and that the corresponding eigenvalue is $-\alpha_1 r_1$ (recall that the other eigenvalues of the community dynamics are basically unaffected by the satellite species). Hence, for small α_1, the satellite species contributes a small eigenvalue (in absolute value). The eigenvalue might be smaller than the other eigenvalues of the community dynamics, in which case the satellite species determines asymptotic resilience.

Second, assume the satellite species has negative invasion fitness, $\alpha_1 < 0$, so that it is maintained in the community by immigration. Neglecting intraspecific competition (i.e., dropping the N_1^2 term in Eq. (F.1)), we obtain the equilibrium biomass $N_1^* = c_1/(|\alpha_1| r_1)$ and the corresponding eigenvalue $\alpha_1 r_1$. If immigration is very weak (very small c_1), both biomass and eigenvalue can be small. Hence, the satellite species can contribute a weakly negative eigenvalue to the community dynamics, and might even determine asymptotic resilience.

The two cases (positive and negative invasion fitness) are illustrated in Fig. 5. For concreteness, we complement Eq. (F.1) with a simple dynamical equation for the aggregate biomass N_0,

$$\frac{\mathrm{d}N_0}{\mathrm{d}t} = r_0 N_0 \left(1 - \frac{N_0}{K_0}\right). \qquad (F.3)$$
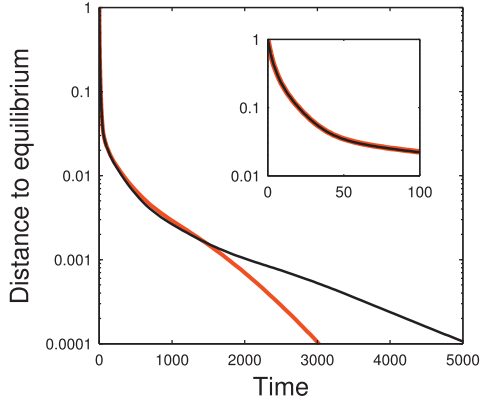
Fig. F.1. Rare species determine asymptotic resilience in random community model. Same model as in Fig. 6, but here we look at a single realization. Black line: recovery trajectory for full community (averaged over perturbation directions). Red line: recovery trajectory for community from which the rarest species has been removed. Inset: zoom of the recovery trajectories for shorter times.

We take $r_0 = 1.0$ and $K_0 = 1.0$, so that $N_0^* = 1.0$ and the associated eigenvalue $\lambda_0 = -1.0$. For the satellite species we set $r_1 = 1.0$ and $\beta_{10} = 0.8$.

In case A of Fig. 5, we take $K_1 = 0.77$ and $c_1 = 0$, so that $\alpha_1 = -0.039$. Hence, the satellite species cannot persist and the community dynamics are not affected.

In case B of Fig. 5, we take $K_1 = 0.83$ and $c_1 = 0$, so that $\alpha_1 = 0.036$. Hence, the satellite species can persist and its equilibrium biomass is $N_1^* = 0.030$. This introduces a new eigenvalue in the community dynamics, equal to $-0.036 = 0.036\,\lambda_0$, which is strongly dominant. This illustrates the first case discussed above.

In case C of Fig. 5, we take $K_1 = 0.77$ and $c_1 = 0.002$. The satellite species is maintained by immigration and its equilibrium biomass is $N_1^* = 0.027$. The associated eigenvalue $-0.11 = 0.11\,\lambda_0$ is strongly dominant. This illustrates the second case discussed above.

The previous observations can be generalized to many-species communities, as shown in Fig. 6. Here we look more closely at a single model realization (Fig. F.1). In this example, asymptotic resilience can be linked to a single species, because the left eigenvector associated with the dominant eigenvalue is strongly concentrated on a single component. This species is the rarest of the community. When removing this species, asymptotic resilience changes drastically, but the short-term recovery dynamics do not (see inset in Fig. F.1). The same phenomena are observed in a majority of model realizations. In other cases, asymptotic resilience is not as clearly associated with a single rare species.